Structural, electrical and sensing properties of ZnFe₂O₄ nanoceramics synthesized by solid-state reaction method

Enass Ahmad [1] ⓘ ✉, *Rasha Yousef*[2]* ⓘ ✉, *Abla Alzoubi [2]* ⓘ ✉, *Nasser Saad Aldin [2]* ⓘ ✉

[1]Department of Physics, Faculty of Science, Tartous University, Tartous, Syria.
[2]Department of Physics, Faculty of Science, Al-Baath University, Homs, Syria
*Corresponding Author.

Abstract

Metal ferrite nanomaterials have emerged as promising materials for gas sensor fabrication due to their high surface area, which provides a large number of adsorption sites for gas molecules. In this research, a zinc ferrite nanoparticle-based gas sensor was prepared using the solid-state reaction method to achieve high sensitivity and a fast response time. The powder zinc ferrite was annealed at different temperatures within the range (500-700) °C for six hours. The optimum temperature for synthesis was 675°C. The structural properties of the prepared compound were studied using X-ray diffraction. The results showed that the compound crystallizes in a cubic crystal structure and belongs to the space group Fd₃m. The lattice constant was a = 8.3856 Å. The theoretical density of $ZnFe_2O_4$ has been calculated. The average crystallite size of the $ZnFe_2O_4$ compound was calculated using Scherrer's formula. The average crystallite size was 29.5 nm. The morphology of the $ZnFe_2O_4$ nanoparticles was observed by scanning electron microscopy. The electrical resistance variations of the $ZnFe_2O_4$ compound were studied as a function of temperature. The electrical resistance values decreased with increasing temperature, indicating semiconducting behavior. The sensing properties of $ZnFe_2O_4$-based sensors were studied. The sensing results showed that the compound is a good sensor for ethanol vapor, where the response and recovery times were 10.115 s and 81.351 s at an operating temperature of 275 °C for a 100 ppm concentration of ethanol. For acetone vapor, the response and recovery times were 10.978 and 102.543 s at an operating temperature of 300 °C for a 100 ppm concentration. Findings indicate that the gas sensor based on zinc ferrite nanoparticles exhibited a high sensitivity and fast response time to ethanol vapor at a relatively low operating temperature 275 °C. These findings suggest future work on the nanostructure of zinc ferrite for its potential use in gas sensing applications.

Keywords: Average crystallite size, Gas sensor, Response and recovery times, Sensitivity, Zinc ferrite.

Introduction

The world is witnessing a remarkable evolution in electronics and industrial equipment, which leads to gaseous wastes that cause environmental pollution and have negative effects on human health[1-4]. This has led to continuous research to discover new materials for detecting gases and their vapors. This has prompted researchers to discover new materials that contribute to the detection process, including binary metal oxide semiconductor materials, which have attracted the attention of many scientists owing to the remarkable progress made in electronic devices based on metal oxides[5-7]. The most important

of these metal oxides are the ferrite metal oxides of the spinel structure, which are formed by the mixing of iron oxide with a divalent metal oxide. The general formula of these materials is $M^{2+}[Fe_2^{3+}]O_4^{2-}$, where M^{2+} is a divalent metal ion. The type of ferrite depends on the location of the metal ion in the tetrahedral or octahedral sites. Normal ferrite given by the formula $M^{2+}[Fe_2^{3+}]O_4^{2-}$, where M^{2+} occupies the A sites and Fe^{3+} occupies the B sites. Inverse ferrite given by the formula $Fe^{3+}[M^{2+}Fe^{3+}]O_4^{-}$, where M^{2+} occupies the B sites and Fe^{3+} occupies both the A and B sites. Mixed spinel ferrite is A mixture of cations of two divalent metals distributed between both sites[8, 9, 10].

Ferrite materials possess important physical and chemical properties that have led to their widespread use in a wide range of applications, including magnetic devices, high-frequency devices, electronics, circuits, catalysts, and high-power magnetic memories[11,12,13]. Additionally, they have been used in the biomedical [14,15,16] and, more recently, due to the increasing demand for gas and vapor detection, they have been extensively used in gas sensors [17,18,19]. This has prompted researchers to study these materials and their properties extensively to exploit them in these applications and to develop and improve them on the nanoscale[18, 20]. Pure spinel ferrite compounds with nanoscale sizes exhibit good sensing properties towards certain gases and vapors[19, 21, 22], especially ethanol and acetone vapors, due to their large surface area to volume ratio and active surface sites that contribute to the gas vapor sensing process.
Zinc ferrite nanoparticles are considered one of the most important normal spinel ferrite materials[22, 23].
Fig 1 represents its crystal structure and the distribution of ions on the octahedral and tetrahedral sites of the lattice[1]. It is an n-type semiconductor metal oxide with high magnetic permeability[25] and a narrow band gap 1.92eV [24-26]. In addition, it exhibits phase stability[13, 24, 27] and high electrical conductivity[23], making it a promising material for use in gas sensing applications, magnetic devices, and in the biomedical field[28, 29].
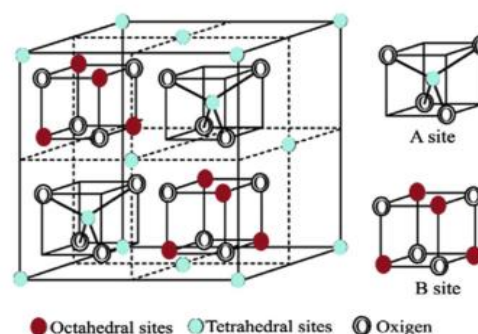

Figure 1. The crystal structure of zinc ferrite1

M. Maharjan et al. prepared zinc ferrite nanoparticles by the citrate-gel method with an average grain size in the range (25-30) nm., they studied the sensing properties of the prepared material towards acetone and ethanol vapors, and the study showed excellent sensing properties at an operating temperature of 350°C[30].
Ya Li Cao et al. also prepared zinc ferrite compounds by the solid-state synthesis method at room temperature conditions and in the presence of PEG600 solution. The prepared material was tested as a gas sensing material for 9 gases, and the study showed the best sensitivity to ethanol and H_2S gas at 332°C and 240°C receptively[5].
Chen et al. prepared four types of spinel ferrites with the formula MFe_2O_4 ; $M(Cu, Zn, Cd, and Mg)$ by the chemical co-precipitation method in the form of powder. The prepared samples were tested as gas sensing materials towards H_2, CO, LPG, C_2H_2 and C_2H_5OH gases. The study showed that the zinc ferrite had the best sensitivity at 350°C, and the sensors showed the best performance towards alcohol, acetone, acetylene, and LPG[31].
Kapse V.D. synthesized nanocompounds with the formula MFe_2O_4 ; $(M: Zn, Ni, Mg)$ with an average grain size in the range (8-35) nm. The prepared materials were tested for the alcohol, ammonia, LPG and H_2S gases. The study showed that the magnesium ferrite compound exhibits a higher response and good selectivity and fast response and recovery times for ethanol at 325°C compared to other gases[3].
Abdullah M. Al-Enizi et al. prepared W-substituted zinc ferrite, with nominal compositions of $ZnFe_{2-2x}W_xO_4$ ($0.0 \leq x \leq 0.15$) by sol–gel technique. Among all the synthesized samples, the $0.15W\text{-}ZnFe_2O_4$ NPs demonstrated the highest sensitivity towards acetone gas at 350 °C[32].
M.I. Nemufulwi et al. synthesized $ZnFe_2O_4$ nanoparticles (NPs) as a volatile organic compound

sensing platform derived from a microwave-assisted hydrothermal method using KOH, NH4OH, and LiOH as base precursors. Findings pointed out that the $ZnFe_2O_4$ NPs sensor based on the NH4OH base precursor with the largest particle size demonstrated the highest gas sensing capabilities as well as improved selectivity to 40 ppm ethanol at 220 °C and good reproducibility[33].

This research aims to prepare a zinc ferrite nanosensor and study its structural and electrical properties, as well as its sensing properties towards ethanol and acetone vapors to determine the best operating temperature and selectivity of the sensor to these vapors.

Materials and Methods

The $ZnFe_2O_4$ compound was prepared by solid-state reaction method, which involves mechanical mixing of the two primary nano oxides, ZnO (99% VWR International Ltd.) and Fe_2O_3 (99.99%, M/s Sigma Aldrich. Ltd) in a weight ratio of 1:1 based on the Eq 1

$$ZnO + Fe_2O_3 \rightarrow ZnFe_2O_4 \qquad \dots\dots\dots 1$$
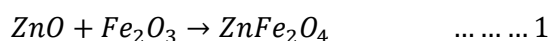
Initially, 1.688g of zinc oxide and 3.312 of iron oxide were weighed to prepare a 5g sample of zinc ferrite in a 1:1 mole ratio based on Eq 1. 1ml of acetone is added to the mixture during the grinding process, which is carried out in a pestle mortar. The grinding process is repeated at least three times to obtain the best homogeneity of the mixture. The grinding process continues until the acetone dries each time. The resulting powder was then dried by heating it to 100°C for some time to remove moisture. Then, the powder was placed in a porcelain crucible and annealed at different temperatures within the range (500-700) °C for six hours. The prepared samples were characterized by X-ray diffraction (XRD) technique (Philips-PW-1840, $\lambda_{Cok_\alpha} = 1.7889 A°$) to study their crystal structure. The morphology of the $ZnFe_2O_4$ nanoparticles was observed by scanning electron microscopy (SEM).

After preparing zinc ferrite nanoparticles, the powder was then pressed using a hydraulic press into pellets with a pressure of ($10ton/m^2$) and a radius of 0.5cm. Copper wires were shaped into electrodes and coated with silver to improve conductivity. The

temperatures were measured using a thermal sensor placed inside an electric heating furnace connected to a computer program to measure the temperature. Fig 2 shows the device used to measure the electrical resistance as a function of temperature.

Figure 2. The electrical measurement device.

The sensing properties are measured in the laboratory by gas sensor sensitivity measurement apparatus. The gas sensor is placed in the measurement chamber. The gas source is turned on and the gas flow is adjusted to the desired level to expose the zinc ferrite gas sensor to the desired gas for a period of time. Fig 3 shows the gas sensing apparatus.

Zinc ferrite can be prepared by several methods, including the sol-gel method[3], hydrothermal synthesis[8], the co-precipitation method[16], the solution combustion synthesis, and the solid-state reaction method[5,29]. Solid-state reaction is a common method for synthesizing ferrite materials and substituting one element for another because it is easy to work with it. It involves grinding high-purity primary materials that are part of the compound to be formed in the required weight ratios and mixing them to obtain a chemically homogeneous mixture using simple preparation equipment. It does not take a long time to obtain the desired compound, and it is also low-cost[5,29].

Figure 3. The gas sensing apparatus.

The sensor sensitivity is determined by the Eq 2[22, 29, 34]

$$S = \frac{R_a}{R_g} \ldots \ldots \ldots 2$$

For the n-type of semiconductor material, where R_a represents the resistance in the presence of air and R_g represents the resistance in the presence of test gas. The sensitivity of the sensor is determined by the type of semiconductor material (n or p type) and the type of gas (reducing or oxidizing).

Results and Discussion

Structural properties

The $ZnFe_2O_4$ compound that prepared by mixing of the starting ZnO and Fe_2O_3 oxides was annealed at different temperatures within the range of 500°C to 700°C to determine the optimum temperature of synthesis for this compound. Fig 4 shows the XRD patterns of $ZnFe_2O_4$, which were annealed in the rang 500°C to 700°C for 6 hours.
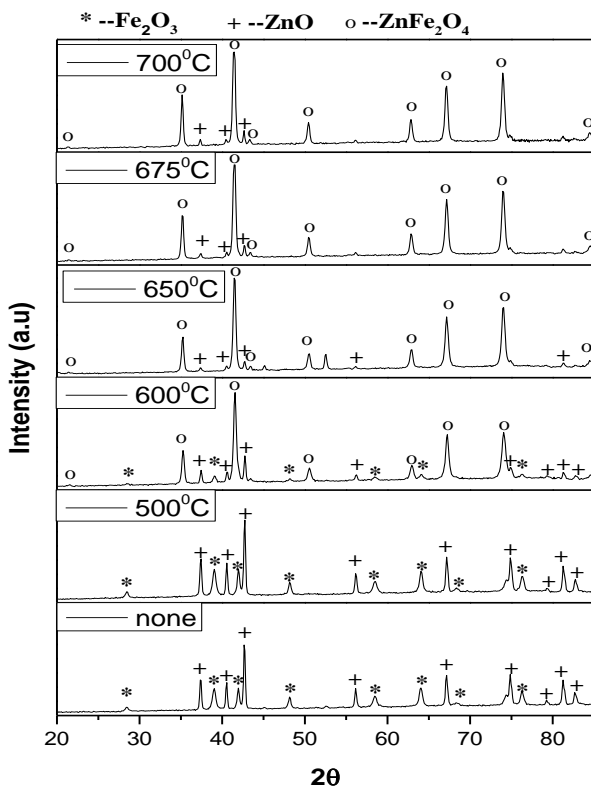
All the diffraction peaks are indexed and compared with the standard JCPDS data of the starting ZnO and Fe_2O_3 oxides and $ZnFe_2O_4$ compound of the numbers 36-1451, 33-0664 and 22-1012 respectively. It was found from Fig. 4, that the most intensive diffraction peaks were attributed to the $ZnFe_2O_4$ compound for the sample annealed at 675°C, where the reaction between primary materials was completed approximately. This indicates that the optimum temperature for $ZnFe_2O_4$ compound synthesis is 675°C. Fig 5 shows the XRD pattern of $ZnFe_2O_4$, which was annealed at 675°C for 6 hours because that is the optimum temperature for $ZnFe_2O_4$ compound synthesis.
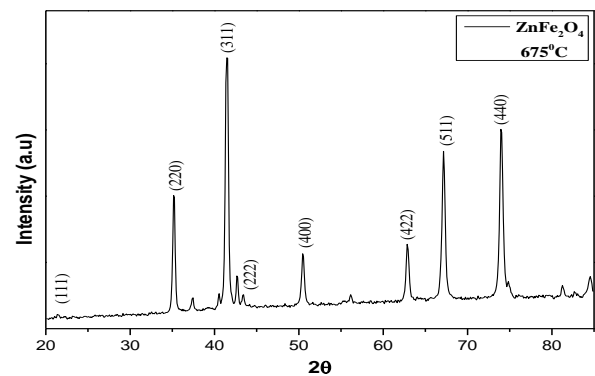
Figure 5. XRD pattern of $ZnFe_2O_4$ compound annealed at 675°C.

Miller indices of diffraction peaks were determined for $ZnFe_2O_4$ compound. These peaks indicate that the $ZnFe_2O_4$ has a cubic structure and belongs to the space group Fm3m. From X-ray diffraction measurements of $ZnFe_2O_4$, the distance between crystal lattices d were calculated using Bragg's law[35]: $n\lambda = 2d \sin\theta$, where $\lambda = 1.7889 A°$ is the x-ray

Figure 4. XRD patterns of the prepared and annealed samples at different temperatures.

wavelength and θ is the diffraction angle. Then the values of the lattice constant are determined using the relation of the distance between parallel crystal plans in the case of the cubic crystal structure that is given by the Eq 3[36]:

$$d_{hkl}^2 = \frac{a^2}{h^2 + k^2 + l^2} \quad \text{……… 3}$$

Where a is lattice constant. The values of the distance between parallel crystal plans and lattice constant of $ZnFe_2O_4$ for each diffracting peak are presented in Table 1.

Table 1. Diffraction peaks, inter planar distances, lattice constant, broadening of diffraction peaks, crystallite size and Miller indices.

2θ	$d_{hkl}(°A)$	$a\ (°A)$	$\beta(°)$	$D(nm)$	(hkl)
21.375	4.823	8.3540	0.5904	15.9	(111)
35.188	2.959	8.3698	0.2952	32.8	(220)
41.466	2.527	8.3800	0.2952	33.4	(311)
43.391	2.420	8.3819	0.2952	33.6	(222)
50.486	2.097	8.3898	0.3936	25.9	(400)
62.889	1.715	8.4000	0.2952	36.6	(422)
67.169	1.617	8.4023	0.2952	37.5	(511)
74.010	1.486	8.4068	0.2952	39.1	(440)

The average lattice constant of $ZnFe_2O_4$ was listed in table 2 and its value was found to agree with the study of Abbas et al[37]. The unit cell volume was also calculated by the Eq 4[38]:

$$V = a^3 \quad \text{……… 4}$$

The unit cell volume of zinc ferrite is listed in table 2. The crystallite size of the $ZnFe_2O_4$ compound was calculated using Scherrer's Eq 5 [39, 40]:

$$D = \frac{0.9\lambda}{\beta cos\theta} \quad \text{……… 5}$$

Where β is the full width at half-maximum (FWHM) of diffraction peaks (radian), λ is the x-ray wavelength ($1.78897A°$) and θ is the Bragg's angle. The estimated values of crystallite size for each diffracting peak of $ZnFe_2O_4$ compound are listed in Table 1. The average crystallite size was 29.5nm, so the prepared compound had nanostructure. The theoretical X-ray density for prepared zin ferrite has been calculated by the Eq 6[41]:

$$\rho_{th} = \frac{ZM}{N_A V} \quad \text{……… 6}$$

Where Z is number of formulae in the unit cell and it is 8 for the spinel lattice, M is molecular weight of the zinc ferrite, N_A is Avogadro's number and V is unit cell volume. The theoretical X-ray density of $ZnFe_2O_4$ compound was listed in table 2.

Table 2. Lattice constant, unit cell volume, grain size, theoretical density and activation energy of $ZnFe_2O_4$ compound.

$a(°A)$	$V(°A^3)$	$D(nm)$	$\rho_{th}(^{gr}/_{cm^3})$	$E_a(eV)$
8.3856	589.6547	29.5	5.43	0.875

The morphology of the $ZnFe_2O_4$ nanoparticles was observed by scanning electron microscopy (SEM). Fig 6 shows the SEM image of $ZnFe_2O_4$ nanoparticles that prepared by solid state reaction. It can be seen from fig 6 the agglomeration of the nanoparticles which consisting of nano fine crystallites with spherical shapes.
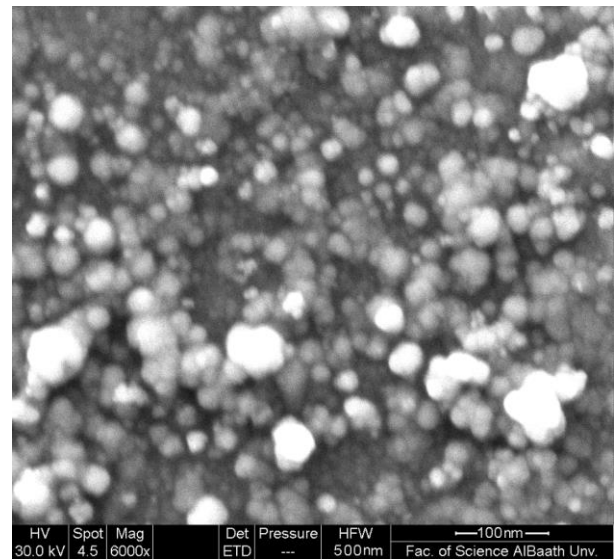

Figure 6. The SEM image of $ZnFe_2O_4$ nanoparticles.

Electrical properties

The electrical resistance variations of $ZnFe_2O_4$ compound were studied as a function of temperature within the range $(470 - 700)°K$. Fig 7 shows electrical resistance variations of $ZnFe_2O_4$ compound as a function of temperature.
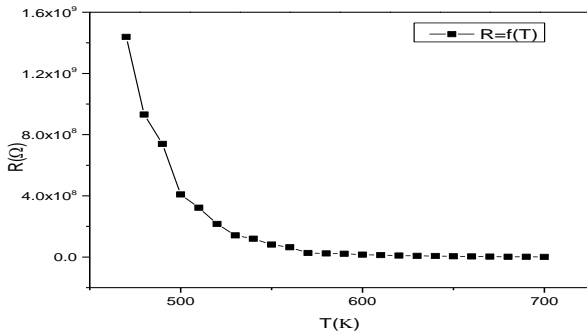
Figure 7. Electrical resistance variations of ZnFe2O4 compound as a function of temperature.

It was found from Fig 7 that the electrical resistance values decreased with increasing temperature, indicating semiconducting behavior within the studied thermal range. The decrease in resistance with increasing temperature is attributed to the increased mobility of charge carriers. Conductivity in ferrites mainly occurs due to hopping between Fe^{2+} and Fe^{3+} ions at octahedral sites, and the probability of this hopping depends on the inter-ionic distance and the activation energy associated with the mobility of charge carriers[12]. To extract the activation energy, the data were analyzed by Eq 7[42, 43]:

$$R = R_0 \exp\left(\frac{E_a}{k_B T}\right) \dots \dots \dots 7$$

Where R is electrical resistance at T temperature, R_0 is electrical resistance at T_0 temperature, E_a is the activation energy, T is the absolute temperature and K_B is the Boltzmann constant. Fig 8 shows variation of $\ln(R)$ as a function of $1/T$ for $ZnFe_2O_4$ compound.
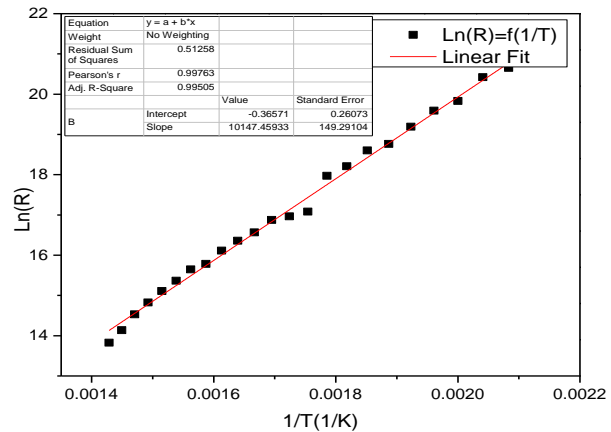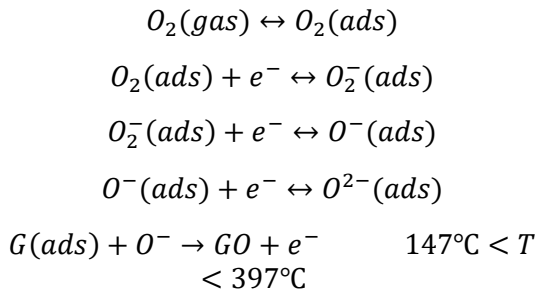

Figure 8. Variation of $\ln(R)$ as a function of $1/T$ for ZnFe₂O₄ compound.

The value of activation energy E_a was calculated from the slope of $\ln(R)$ versus $1/T$ plot. The calculated value of activation energy is $E_a = 0.875 eV$.

Sensing properties

In this work the sensitivity of zinc ferrite nanoparticles was investigated to ethanol and acetone vapors within 175-400 °C range. The electrical resistance variation of the zinc ferrite-based sensor was studied as a function of temperature to determine the sensor's operating temperature, sensitivity and response and recovery times. When a zinc ferrite-based sensor is exposed to air, oxygen molecules are adsorbed on the sensor surface. These adsorbed oxygen molecules capture free electrons from the conduction band to form oxygen anions[34, 44, 45]. The formation of these anions depends on the operating temperature. At low operating temperatures (below 147°C), oxygen anions O_2^- transferred to O^-. With increasing temperature, these oxygen ions transform into O^{2-} and an electron depletion layer (n-type) is formed on the semiconductor surface due to the loss of electrons. This results in an increase in the resistance of sensor material[1, 24, 29]. When the sensing material is exposed to the target gas, the depletion region decreases, which in turn decreases the resistance of the sensing material. The resistance reaches its optimal value with increasing operating temperature. When oxygen adsorption and desorption reach a dynamic equilibrium, the sensor exhibits a maximum response to the target gas[1, 29]. The transfer of electrons from the conduction band of zinc ferrite to adsorbed
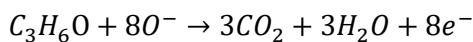
oxygen molecules can be expressed according to the following reactions:

$$O_2(gas) \leftrightarrow O_2(ads)$$

$$O_2(ads) + e^- \leftrightarrow O_2^-(ads)$$

$$O_2^-(ads) + e^- \leftrightarrow O^-(ads)$$

$$O^-(ads) + e^- \leftrightarrow O^{2-}(ads)$$

$$G(ads) + O^- \rightarrow GO + e^- \qquad 147°C < T < 397°C$$

The last equation was written in the presence of vapors as following: In the presence of ethanol vapor[1]

$$C_2H_5OH + 6O^- \rightarrow 2CO_2 + 3H_2O + 6e^-$$
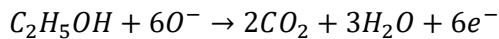
While in the presence of acetone vapor[1, 24, 46]

$$C_3H_6O + 8O^- \rightarrow 3CO_2 + 3H_2O + 8e^-$$

The sensitivity of the gas is affected by the operating temperature of the sensor, the concentration of the gas and the humidity, in addition to factors related to the morphology of the prepared zinc ferrite compound such as the specific surface area, the contact area, the porosity, the particle size, and the agglomeration. The characteristic properties of the spinel structure of zinc ferrite have contributed to its good sensitivity to the studied vapors. Fig 9 shows the sensitivity of zinc ferrite nanoparticles to temperature change for both ethanol and acetone vapors at a concentration of 100 ppm.
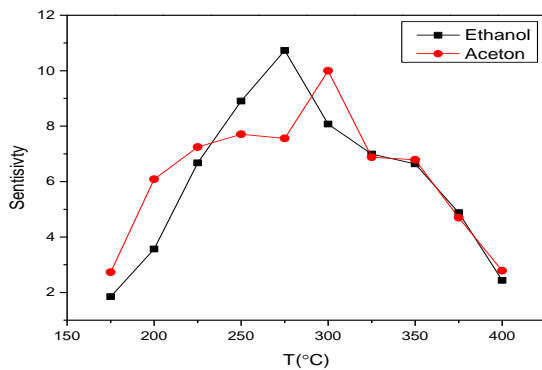
Figure 9. Sensitivity of zinc ferrite nanoparticles to ethanol and acetone vapors at a concentration of 100 ppm.

It was obvious from Fig 9, that the operating temperature of the prepared zinc ferrite sensor for a concentration of 100 ppm of ethanol vapor is equal to 275°C, and the sensitivity value was recorded as 10.731. It is noted that at this temperature, the reaction rate between the gas molecules and the adsorbed oxygen and the surface of the nanoparticle is very large. Therefore, the gas molecules can overcome the energy barrier and interact with the surface of the particle, and we obtain the best operating temperature for the sensor[47]. The sensitivity value was recorded for the same amount of acetone vapor and this 10 at an operating temperature of 300°C, as shown in Fig 9. Fig 10 shows the gas response curve as a function of time on consecutive exposure to 100 ppm ethanol vapor with 3 cycles at 275°C.
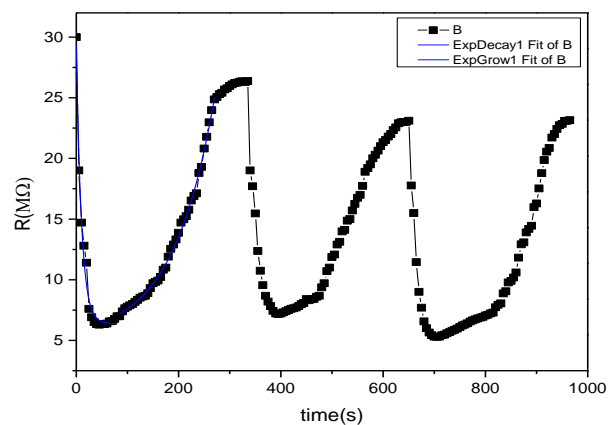
Figure 10. The response curve as a function of time of ZnFe$_2$O$_4$ sensor on consecutive exposure to 100 ppm ethanol vapor with 3 cycles at 275°C (Reproducibility).

It is observed from Fig 10 that the prepared ZnFe$_2$O$_4$ sensor has good reproducibility after being exposed to ethanol vapor for three consecutive times. The response and recovery times of ZnFe$_2$O$_4$ sensor to 100 ppm ethanol vapor were determined by doing an exponential fit to the response data for the first cycle. The values of response and recovery times are listed in table 3. Fig 11 shows the gas response curve as a function of time on consecutive exposure to 100 ppm acetone vapor with 3 cycles at 300°C.
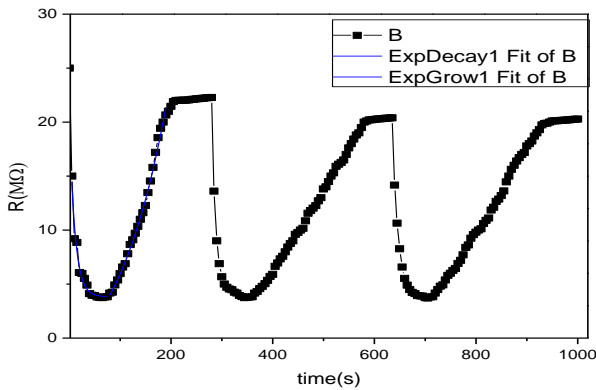
Figure 11. The response curve as a function of time of ZnFe$_2$O$_4$ sensor on consecutive exposure to 100 ppm acetone vapor with 3 cycles at 300℃ (Reproducibility).

The response and recovery times of ZnFe$_2$O$_4$ sensor to 100 ppm acetone vapor were determined and listed in table 3. The concentration of ethanol vapor was increased to 150 ppm and 200 ppm, and an increase in the sensitivity of the prepared gas sensor was observed with increasing ethanol vapor concentration. Fig 12 shows the sensitivity curve as a function of temperature at different concentrations of ethanol vapor.
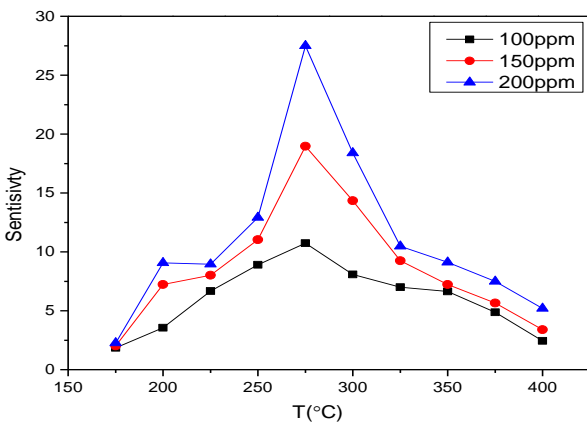

Figure 12. The sensitivity curve as a function of temperature at different concentrations of ethanol vapor.

The sensitivity curve for acetone vapor at different concentrations was also plotted in Fig 13.
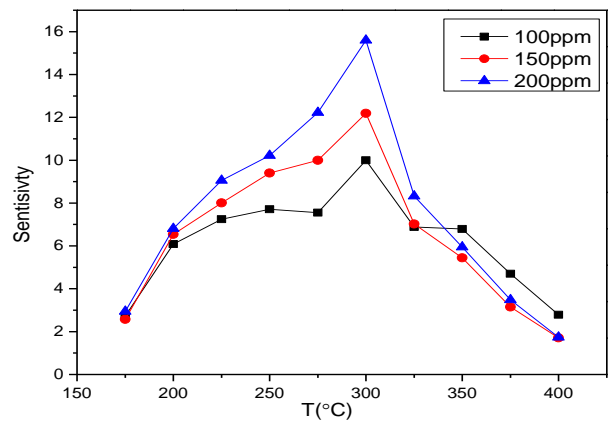
Figure 13. The sensitivity curve as a function of temperature at different concentrations of acetone vapor.

Table 3. Working temperature, Sensitivity, Response time and recovery time of ZnFe2O4 compound for 100 ppm of ethanol and acetone vapors.

Target vapors	T(℃)	Sensitivity	Response time (s)	recovery time (s)
ethanol	275	10.73	10.12	81.35
acetone	300	10	10.98	102.54

A linear fitting was done for the sensitivity with different concentrations. It was observed that the sensitivity of the studied vapors increased with increasing vapor concentration as shown in Figs 14 and 15. This is attributed to the increased number of active sites that it is reacting with in the gas vapor.

Figure 14. The sensitivity as a function ethanol vapor concentrations.

Figure 15. The sensitivity as a function acetone vapor concentrations.

The table shows a comparison of the results of this work with some of the scientific work related to this work
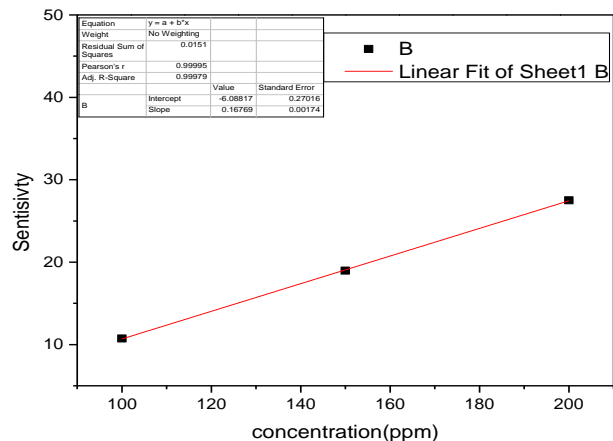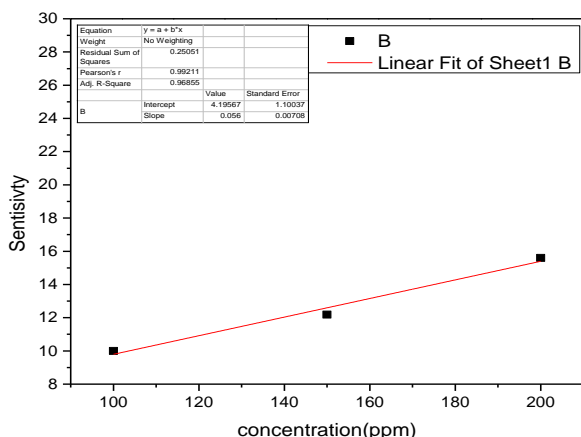
Table 3. A comparison of the results of this work with some of the scientific work related to this work.

Materials	Materials preparation	Annealing Temperature	Target gas	Sensitivity	Operation temperature	Response time	Recovery time	ref
ZnFe₂O₄ powders (50 ppm)	Crited Sol-gel	600℃	ethanol	9.1	325℃	40s	72s	[3]
ZnFe₂O₄ film (100 ppm)	Solid state	< 100℃	ethanol	21.5	332℃	4s	14s	[5]
Bulk ZnFe₂O₄ film (100 ppm)	Solid state	< 100℃	ethanol	5.1	325℃	25s	70s	[5]
ZnFe₂O₄ powders (1000 ppm)	Solid state	600℃	ethanol	29.1	300℃	5s	18s	[29]
ZnFe₂O₄ nanoparticles (100ppm)	hydrothermal	400℃	ethylene glycol	10.2	160℃	53s	65s	[22]
ZnFe₂O₄ nanoparticles (10ppm) acetone	solvothermal	400℃	acetone	3.20	175℃	60s	231s	[48]
ZnFe₂O₄ powders (30 ppm)	hydrothermal	180 − 550℃	acetone	26	200℃	19s	35s	[28]
ZnFe₂O₄ powders (100 ppm)	Solid state	675℃	ethanol	10.73	275℃	10.12	81.35	This work
ZnFe₂O₄ powders (100 ppm)	Solid state	675℃	acetone	10	300℃	10.98	102.54	This work

Conclusion

Zinc ferrite nanoparticles were synthesized from zinc ferrite using the solid-state synthesis method as a Nano gas sensing material for both ethanol and acetone vapors. X-ray diffraction analysis showed that the prepared compound was obtained at a calcination temperature of 675 °C and with an average crystallite size of 29.5 nm. Scanning electron microscopy (SEM) confirmed the nanostructure of zinc ferrite. The sensitivity results showed that the prepared sensor exhibits higher sensitivity to ethanol vapor at a lower operating temperature T = 275 °C.

This is attributed to the higher number of active sites, the natural spinel structure of zinc ferrite nanoparticles, the electrical conduction mechanism involving electron hopping between Fe^{2+} and Fe^{3+} ions, their distribution on the tetrahedral sites in the spinel structure, and the lower operating temperature. Also, the gas sensor based on zinc ferrite nanoparticles showed a fast response and recovery time of 10.12 s and 81.35s for ethanol vapor, and revealed higher stability over 3 cycles.

This finding makes it a candidate for gas sensor applications involving ethanol vapor.

Acknowledgment

Authors' Declaration

- Conflicts of Interest: None.
- We hereby confirm that all the Figures and Tables in the manuscript are ours. Furthermore, any Figures and images, that are not ours, have been included with the necessary permission for re-publication, which is attached to the manuscript.

- No animal studies are present in the manuscript.
- No human studies are present in the manuscript.
- Ethical Clearance: The project was approved by the local ethical committee at Al-Baath University, Homs, Syria.

Authors' Contribution Statement

E.A. worked at conceptualization, analysis, editing and original draft preparation. R.Y. validation, reviewing, editing, and data curation. A.A. methodology, software use, writing, and supervision.

N.S.D. visualization, investigation, and supervision. All authors have read and agreed to the published version of the manuscript.

References

1. Wu K, Li J, Zhang C. Zinc ferrite based gas sensors: A review. Ceram Int. 2019; 45 (9) : 11143-11157. https://doi.org/10.1016/j.ceramint.2019.03.086
2. Kumar S, Bharti B, Zha X, Ouyang F, Ren P. Recent Development in Industrial Scale Fabrication of Nanoparticles and Their Applications. In Liquid and Crystal Nanomaterials for Water Pollutants Remediation. CRC Press. 2022 Jul 7; 88-118.
3. Kapse VD. Preparation of nanocrystalline spinel-type oxide materials for gas sensing applications. Res. J. Chem. Sci. 2015. 5(8): 7-12. https://doi.org/2ISCA-RJCS-2015-093
4. He H, Li X, Li S, Zhu W, Jiang R, Zhai Z, et al. Utilizing oxygen-rich vacancies in Bi2O2CO3/ZnFe2O4 heterojunction photocatalytic materials for the efficient degradation of tetracycline hydrochloride in water. J Water Process Eng. 2024 Aug 1; (65):105742. https://doi.org/10.1016/j.jwpe.2024.105742
5. Cao Y, Jia D, Hu P, Wang R. One-step room-temperature solid-phase synthesis of ZnFe2O4 nanomaterials and its excellent gas-sensing property. Ceram Int. 2013; 39(3): 2989-2994. https://doi.org/10.1016/j.ceramint.2012.09.076
6. Aslam A, Rehman AU, Amin N, Amman M, Akhtar M, Morley NA, et al. To study the structural, electrical, and magnetic properties of M (M= Mg2+, Mn2+, and Cd2+) doped Cu-Ni-Co-La spinel ferrites. Mater Chem Phys 2023 Jan; 15(294): 127034. https://doi.org/10.1016/j.matchemphys.2022.127034
7. Nemufulwi MI, Swart HC, Mhlongo GH. Advances of Nano-Enabled ZnFe2O4 Based-Gas Sensors for VOC Detection and Their Potential Applications: A Review. Processes (Basel). 2023 Oct 31; 11(11): 3122. https://doi.org/10.3390/pr11113122
8. Zhang J, Song J M, Niu H L, Mao C J, Zhang S Y, Shen Y H. ZnFe$_2$O$_4$ nanoparticles: Synthesis, characterization, and enhanced gas sensing property for acetone. Sens Actuators B Chem. 2015; 221: 55-62. http://dx.doi.org/10.1016/j.snb.2015.06.040
9. Abdulhamid ZM, Dabbawala AA, Delclos T, Straubinger R, Rueping M, Polychronopoulou K, et al. Synthesis, characterization, and preliminary insights of ZnFe2O4 nanoparticles into potential applications, with a focus on gas sensing. Sci Rep. 2023 Nov 11; 13(1): 19705. https://doi.org/10.1038/s41598-023-46960-w
10. Malaescu I, Sfirloaga P, Marin CN, Bunoiu MO, Vlazan P. Experimental Investigations on the Electrical Conductivity and Complex Dielectric Permittivity of ZnxMn1− xFe2O4 (x= 0 and 0.4) Ferrites in a Low-Frequency Field. Crystals (Basel).

2024 May 4; 14(5): 437. https://doi.org/10.3390/cryst14050437

11. Muaawia AZ, Mujtaba A, Khan MI, Ali B, Karamat A, Asghar A. Enhanced medicinal applications of Co-doped Zn0. 5Ni0. 5Fe2-xO4 for (X= 0.00 and 0.0250) soft ferrites: A structural analysis. J Appl Math. 2023 Aug 5; 1(2): 237. https://doi.org/10.59400/jam.v1i2.237

12. Gabal M A, Katowah D F, Hussein M A, Al-Juaid A A, Awad A, Abdel-Daiem A M, et al. Structural and Magnetoelectrical Properties of MFe_2O_4 (M= Co, Ni, Cu, Mg, and Zn) Ferrospinels Synthesized via an Egg-White Biotemplate. ACS omega. 2021; 6(34): 22180-22187. https://doi.org/10.1021/acsomega.1c02858

13. Dippong T, Levei E A, Cadar O. Recent advances in synthesis and applications of MFe_2O_4 (M= Co, Cu, Mn, Ni, Zn) nanoparticles. Nanomater. 2021; 11(6): 1560. https://doi.org/10.3390/nano11061560

14. Tabesh F, Mallakpour S, Hussain CM. Recent advances in magnetic semiconductor ZnFe2O4 nanoceramics: History, properties, synthesis, characterization, and applications. J Solid State Chem. 2023; (322): 123940. https://doi.org/10.1016/j.jssc.2023.123940

15. Prajapat P, Dhaka S, Mund H S. Investigation of the influence of annealing temperature on the structural and magnetic properties of $MgFe_2O_4$. J Electron. Mater. 2021; 50(8): 4671-4677. https://doi.org/10.1007/s11664-021-09022-3

16. Andhare D D, Jadhav S A, Khedkar M V, Somvanshi S B, More S D, Jadhav K M. Structural and chemical properties of $ZnFe_2O_4$ nanoparticles synthesised by chemical co-precipitation technique. J Phys Conf Ser. 2020; 1644(1): 012014. http://dx.doi.org/10.1088/1742-6596/1644/1/012014

17. Abd-Elkader O, Al-Enizi AM, Shaikh SF, Ubaidullah M, Abdelkader MO, Mostafa NY. The Structure, Magnetic, and Gas Sensing Characteristics of W-Substituted Co-Ferrite Nanoparticles. Crystals (Basel). 2022 Mar 14; 12(3): 393. https://doi.org/10.3390/cryst12030393

18. Manoharan C, Bououdina M, Venkateshwarlu M, Murugan A. Enhanced magnetic, electrochemical and gas sensing properties of cobalt substituted nickel ferrite nanoparticles prepared by hydrothermal route. J Phys Chem Solids.2023. 178; 111364. https://doi.org/10.1016/j.jpcs.2023.111364

19. Bhagat B, Gupta S K, Mandal D, Badyopadhyay R, Mukherjee K. Autocombustion Route Derived Zinc Ferrite Nanoparticles as Chemiresistive Sensor for Detection of Alcohol Vapors. ChemPhysChem. 2024; e202300730. https://doi.org/10.1002/cphc.202300730

20. Xavier S, Jose D, George S, Alekha KV. Structural and magnetic characterization of transition metal substituted ferrite nanoparticles. AIP Conf. Proc. 2020 Sep 7; 2263(1). https://doi.org/10.1063/5.0017047

21. Haija MA, Chamakh M, Othman I, Banat F, Ayesh AI. Fabrication of H 2 S gas sensors using Zn x Cu 1-x Fe 2 O 4 nanoparticles. Appl Phys A Mater Sci Process. 2020 Jul; 126: 1-9. https://doi.org/10.1007/s00339-020-03661-9

22. Husain S, Yusup M, Haryanti NH, Saukani M, Arjo S, Riyanto A. Characteristics of zinc ferrite nanoparticles (ZnFe 2O4) from natural iron ore. IOP Conf Ser Earth Environ Sci. 2021 Apr 1; 758(1): 012001. https://doi.10.1088/1755-1315/758/1/012001

23. Wen Z, Ren H, Li D, Lu X, Joo S W, Huang J. Ahighly efficient acetone gas sensor based on 2D porous $ZnFe_2O_4$ nanosheets. Sens Actuators B Chem. 2023; 379: 133287. https://doi.org/10.1016/j.snb.2023.133287

24. Wu K, Lu Y, Liu Y, Liu Y, Shen M, Debliquy M, et al. Synthesis and acetone sensing properties of copper (Cu2+) substituted zinc ferrite hollow micro-nanospheres. Ceram Int. 2020; 46(18): 28835-28843. https://doi.org/10.1016/j.ceramint.2020.08.049

25. De Oliveira R C, Ribeiro R P, Cruvinel G H, Amoresi R C, Carvalho M H, De Oliveira A J A, et al Role of surfaces in the magnetic and ozone gas-sensing properties of ZnFe2O4 nanoparticles: theoretical and experimental insights. ACS Appl. Mater. Interfaces. 2021; 13(3): 4605-4617. https://dx.doi.org/10.1021/acsami.0c15681

26. Tahir W, Zeeshan T, Waseem S, Ali MD, Kayani Z, Aftab ZE, et al. Impact of silver substitution on the structural, magnetic, optical, and antibacterial properties of cobalt ferrite. Sci Rep. 2023 Sep 21; 13(1): 15730. https://doi.org/10.1038/s41598-023-41729-7

27. Sun B, Zhang X, Zhou G, Zhang C, Li P, Xia Y, et al. affect of Cu ions assisted conductive filament on resistive switching memory behaviors in $ZnFe_2O_4$-based devices. J Alloys Compd. 2017; 694: 464-470. http://dx.doi.org/10.1016/j.jallcom.2016.10.008

28. Guo W, Huang L, Zhao B, Gao X, Fan Z, Liu X, et al. Synthesis of the $ZnFe_2O_4/ZnSnO_3$ nanocomposite and enhanced gas sensing performance to acetone. Sens Actuators B Chem. 2021; 346: 130524. https://doi.org/10.1016/j.snb.2021.130524

29. Cao Y, Qin H, Niu X, Jia D. Simple solid-state chemical synthesis and gas-sensing properties of spinel ferrite materials with different morphologies. Ceram Int. 2016; 42(9): 10697-10703. http://dx.doi.org/10.1016/j.ceramint.2016.03.184

30. Maharajan M, Mursalin M D, Narjinary M, Rana P, Sen S, et al. Synthesis, characterization and vapour sensing properties of nanosized $ZnFe_2O_4$. Trans Ind Ceram Soc. 2014; 73(2): 102-104. http://dx.doi.org/10.1080/0371750X.2014.922421

31. Chen N. S, Yang X. J, Liu E. S, Huang J. L. Reducing gas-sensing properties of ferrite compounds MFe_2O_4 (M= Cu, Zn, Cd and Mg). Sens Actuators B Chem. 2000; 66(1-3): 178-180. https://doi.org/10.1016/S0925-4005(00)00368-3

32. Al-Enizi AM, Abd-Elkader OH, Shaikh SF, Ubaidullah M, Abdelkader MO, Mostafa NY.

Fabrication and Characterization of W-Substituted ZnFe2O4 for Gas Sensing Applications. Coatings. 2022 Sep 17; 12(9): 1355. https://doi.org/10.3390/coatings12091355

33. Nemufulwi MI, Swart HC, Mdlalose WB, Mhlongo GH. Size-tunable ferromagnetic ZnFe2O4 nanoparticles and their ethanol detection capabilities. Appl Surf Sci. 2020 Apr 1; 508: 144863. https://doi.org/10.1016/j.apsusc.2019.144863

34. Njoroge M A, Kirimi N M, Kuria K P. Spinel ferrites gas sensors: a review of sensing parameters, mechanism and the effects of ion substitution. Crit Rev Solid State Mater Sci. 2022; 47(6): 807-836. https://doi.org/10.1080/10408436.2021.1935213

35. Muhammed SA, Abbas NK. Synthesis and investigation of structural and optical properties of CdO: Ag nanoparticles of various concentrations. Baghdad Sci J. 2023, 20(5 Suppl.): 2002-2011. https://dx.doi.org/10.21123/bsj.2023.7292

36. Sathiyamurthy K, Rajeevgandhi C, Bharanidharan S, Sugumar P, Subashchandrabose, S. Electrochemical and magnetic properties of zinc ferrite nanoparticles through chemical co-precipitation method. Chem Data Coll. 2020; 28: 100477. https://doi.org/10.1016/j.cdc.2020.100477

37. Saadon AK, Shaban AH, Jasim KA. Effects of the ferrits addition on the properties of Polyethylene terephthalate. Baghdad Sci J. 2022; 19(1): 208-216. http://dx.doi.org/10.21123/bsj.2022.19.1.0208

38. Andhare DD, Jadhav SA, Khedkar MV, Somvanshi SB, More SD, Jadhav KM. Structural and chemical properties of ZnFe2O4 nanoparticles synthesised by chemical co-precipitation technique. J Phys Conf Ser. 2020 Oct 1; 1644(1): 012014. https://doi:10.1088/1742-6596/1644/1/012014

39. Langford JI, Wilson AJ. Scherrer after sixty years: a survey and some new results in the determination of crystallite size. J Appl Crystallogr. 1978 Apr 1; 11(2): 102-13. https://doi.org/10.1107/S0021889878012844

40. Scherrer P. Bestimmung der Grosse und inneren Struktur von Kolloidteilchen mittels Rontgenstrahlen. Nach Ges Wiss Gottingen. 1918; 2: 8-100.

41. Nitika, Rana A, Kumar V. Investigation on anneal-tuned properties of ZnFe2O4 nanoparticles for use in humidity sensors. Appl Phys A Mater Sci Process. 2021 Aug; 127(8): 609. https://doi.org/10.1007/s00339-021-04755-8

42. Yousef R, Nassif A, Al-Zoubi A, Saad Al-Din N. Synthesis and Characterisation of Structural and Electrical Properties of CuMn2O4 Spinel Compound. Sci J King Faisal Univ. 2022; 22(2): 47-50. https://doi.org/10.37575/b/sci/210028

43. Kolhar P, Sannakki B, Verma M, SV P, Alshehri M, Shah NA. Synthesis, Characterization and Investigation of Optical and Electrical Properties of Polyaniline/Nickel Ferrite Composites. Nanomaterials (Basel). 2023 Jul 31; 13(15): 2223. https://doi.org/10.3390/nano13152223

44. Dong C, Liu X, Xiao X, Du S, Wang Y. Monodisperse ZnFe2O4 nanospheres synthesized by a nonaqueous route for a highly slective low-ppm-level toluene gas sensor. Sens Actuators B Chem. 2017 Feb 1; 239: 12316. https://doi.org/10.1016/j.snb.2016.09.122

45. ZHOU Xin, Highly sensitive acetone gas sensor based on porous $ZnFe_2O_4$ nanospheres. Sens Actuators B Chem. 2015; 206: 577-583. http://dx.doi.org/doi:10.1016/j.snb.2014.09.080

46. Nemufulwi M I, Swart H C, Mhlongo G H. Evaluation of the effects of Au addition into ZnFe2O4 nanostructures on acetone detection capabilities. Mater Res Bull. 2021; 142: 111395. https://doi.org/10.1016/j.materresbull.2021.111395

47. Hamdan SA, Ali IM. Enhancement of Hydrothermally Co3O4 Thin Films as H2S Gas Sensor by Loading Yttrium Element. Baghdad Sci J. 2019 Jan 2; 16(1): 221-9. http://dx.doi.org/10.21123/bsj.2019.16.1(Suppl.).0221

48. Wu K, Luo Y, Li Y, Zhang C. Synthesis and acetone sensing properties of $ZnFe_2O_4$/rGO gas sensors. Beilstein J Nanotechnol. 2019; 10(1): 2516-2526. https://doi.org/10.3762/bjnano.10.242

دراسة الخصائص البنيوية والكهربائية والتحسسية لمساحيق سيراميكية نانوية من ZnFe₂O₄ المصنعة بطريقة تفاعل الحالة الصلبة

ايناس احمد¹، رشا يوسف²، عبلة الزعبي²، ناصر سعد الدين²

¹ قسم الفيزياء، كلية العلوم، جامعة طرطوس، طرطوس، سوريا
² قسم الفيزياء، كلية العلوم، جامعة البعث، حمص، سوريا

الخلاصة

ظهرت المواد النانوية القائمة على فريت المعادن كمواد واعدة في تصنيع الحساسات الغازية بسبب مساحتها السطحية العالية التي توفر عدداً كبيراً من مواقع الادمصاص لجزيئات الغاز . في هذا البحث، تم تحضير حساس غازي نانوي قائم على فريت الزنك باستخدام طريقة تفاعل الحالة الصلبة بهدف تحقيق حساسية عالية وزمن استجابة سريع. تم تلدين مساحيق فريت الزنك المحضر عند درجات حرارة مختلفة ضمن المجال الحراري C°(700-500) لمدة ست ساعات وتبين أن درجة الاصطناع المثلى للمركب C°675. تم دراسة الخصائص البنيوية للمركب المحضر باستخدام تقنية انعراج الأشعة السينية. أظهرت النتائج أن المركب يتبلور وفق بنية بلورية مكعبية وينتمي للمجموعة الفراغية Fd3m. كانت قيمة ثابت الشبكة البلورية لفرايت الزنك Å 8.3856 = a. تم حساب الكثافة النظرية للمركب ZnFe₂O₄. تم حساب حجم الحبيبات للمركب ZnFe₂O₄ باستخدام صيغة شرر. كان متوسط حجم الحبيبات 29.5nm. تم دراسة تغيرات المقاومة الكهربائية لمركب فرايت الزنك ZnFe₂O₄ كتابع لدرجة الحرارة. تناقصت قيم المقاومة الكهربائية مع زيادة درجة الحرارة مما يشير إلى سلوك نصف ناقل للعينة المحضرة. درست الخصائص التحسسية للحساس القائم على ZnFe₂O₄. أظهرت النتائج التحسسية أن الحساس القائم على فريت الزنك هو حساس جيد لبخار الإيثانول بزمن استجابة واسترجاع 10.115s و81.351s على الترتيب عند درجة حرار تشغيل 275 °C من أجل تركيز قدره 100 ppm. وجد أن زمن الاستجابة والاسترجاع لبخار الأسيتون 10.978s و 102.543sعند درجة حرارة تشغيل 300°C من أجل تركيز 100 ppm من بخار الأسيتون.. بينت النتائج أن الحساس الغازي القائم على الجسيمات النانوية من فرايت الزنك حساسية عالية وزمن استجابة سريع لبخار الإيثانول عند درجة حرارة تشغيل منخفضة نسبيا وهي275°C . تقترح هذه النتائج التي تم التوصل إليها إلى العمل المستقبلي على البنية النانوية لفرايت الزنك لاستخدامه في تطبيقات الحساسات الغازية الكامنة.

الكلمات المفتاحية: حجم الحبيبات الوسطي، حساس غازي، أزمنة الاستجابة والاستعادة، الحساسية، فرايت الزنك.